

Benzene Adsorbed on Metals: Concerted Effect of Covalency and van der Waals Bonding

Wei Liu¹, Javier Carrasco², Biswajit Santra^{1,3}, Angelos

Michaelides⁴, Matthias Scheffler¹, and Alexandre Tkatchenko^{1*}

¹*Fritz-Haber-Institut der Max-Planck-Gesellschaft, Faradayweg 4-6, D-14195, Berlin, Germany*

²*Instituto de Catálisis y Petroleoquímica, CSIC, Marie Curie 2, E-28049, Madrid, Spain*

³*Department of Chemistry, Princeton University, Princeton, New Jersey 08544, USA*

⁴*Thomas Young Centre, London Centre for Nanotechnology and Department of Chemistry, University College London, London WC1E 6BT, United Kingdom*

The adsorption of aromatic molecules on metal surfaces plays a key role in condensed matter physics and functional materials. Depending on the strength of the interaction between the molecule and the surface, the binding is typically classified as either physisorption or chemisorption. Van der Waals (vdW) interactions contribute significantly to the binding in physisorbed systems, but the role of the vdW energy in chemisorbed systems remains unclear. Here we study the interaction of benzene with the (111) surface of transition metals, ranging from weak adsorption (Ag and Au) to strong adsorption (Pt, Pd, Ir, and Rh). When vdW interactions are accurately accounted for, the barrier to adsorption predicted by standard density functional theory (DFT) calculations essentially vanishes, producing a metastable precursor state on Pt and Ir surfaces. Notably, vdW forces contribute more to the binding of covalently bonded benzene than they do when benzene is physisorbed. Comparison to experimental data demonstrates that some of the recently developed methods for including vdW interactions in DFT allow quantitative treatment of both weakly and strongly adsorbed aromatic molecules on metal surfaces, extending the already excellent performance found for gas-phase molecules.

I. INTRODUCTION

The adsorption of aromatic molecules at transition-metal surfaces is important for fundamental and applied surface science studies,¹⁻³ and these systems show promise as components in (opto)-electronic devices.⁴ In the case of weak overlap of electron orbitals between the adsorbate and the substrate surface, the ubiquitous van der Waals (vdW) interactions is frequently the only force that binds the molecule to the surface. This situation is typically referred to as physisorption. In the chemisorption case, the covalent or ionic bonding dominates and the effect of vdW interactions on the overall strength of adsorption is typically assumed to be weak. In this study, we challenge this conventional view, by demonstrating the significantly larger contribution of vdW energy to the stabilization of strongly adsorbed benzene on (111) surfaces of Pt, Pd, Rh, and Ir metals when compared to physisorption on Ag(111) and Au(111) surfaces.

Whereas the role of vdW forces in the binding of atoms and molecules in the gas phase is reasonably well understood, at solid surfaces our understanding remains far from complete. Indeed, until recent developments (see, *e.g.*, Refs.⁵⁻⁸) for efficiently incorporating the long-range vdW energy within density functional theory (DFT) calculations it was not possible to determine the role of the vdW energy for extended systems and adsorption processes.⁹⁻¹¹ A large majority of previous theoretical work on vdW interactions mainly focused on weakly bound systems.¹²⁻¹⁸ Typical examples include benzene (Bz) adsorbed on the Ag(111) and Au(111) surfaces,¹⁵⁻¹⁸ and noble gases on the Cu(111), Ag(111), Pt(111), and Pd(111) surfaces.^{10,19-21} A unifying aspect of these studies is the

observation that the inclusion of vdW interactions into standard DFT within the generalized gradient approximation (GGA) often brings a large increase in binding, and results in a much better agreement with experimental adsorption distances and energies. However, the vdW forces can also have a *qualitative* impact on the adsorption process. One particularly interesting example was reported by Blügel's group, showing that the vdW forces are the key ingredient to trigger the binding of pyridine on Cu(110) from physisorption to weak chemisorption.²² Mittendorfer *et al.*²³ reported a novel mechanism for graphene adsorption on Ni(111), where weak covalent and vdW interactions lead to two different minima in the binding curve. Similar results were found by Li *et al.*²⁴ Another example was shown in our recent work on the isophorone molecule (C₉H₁₄O) at the Pd(111) surface, which illustrated that the binding structure and the dehydrogenation pathway in this system can be predicted only after accounting for vdW interactions.²⁵ The vdW interactions were also shown to play a role in the chemisorption of benzene on the Si(100) surface.^{26,27} However, in this case the vdW-DF method leads to a *smaller* adsorption energy than the pure PBE functional,²⁶ while the PBE+vdW method predicts a vdW contribution of 0.5 eV.²⁷

In this work, we demonstrate the significant concerted effect of covalent bonding and vdW interactions for benzene interacting with metal surfaces, leading to qualitative changes in the adsorption behavior when vdW interactions are accurately treated (see Figure 2). In particular, our calculations predict a metastable precursor state for benzene on Pt(111) in agreement with the experimental findings,²⁸ along with a peculiar "phase transition"

behavior of the projected HOMO/LUMO occupations of the benzene molecule. Comparison to experimental data demonstrates that recently developed methods for including vdW interactions in DFT^{8,10} allow quantitative treatment of both weakly and strongly adsorbed aromatic molecules on metal surfaces, extending the already excellent performance found for gas-phase molecules.^{8,29}

II. COMPUTATIONAL METHOD

We used two different vdW-inclusive approaches in the present work: a newly developed PBE+vdW^{surf} method,¹⁰ as implemented in the FHI-aims all-electron code;³⁰ and the optB88-vdW method,⁸ as implemented in the VASP code.^{31,32} The PBE+vdW^{surf} approach includes screened vdW interactions (beyond the pairwise atom-atom approximation) to study adsorbates on surfaces, by a synergetic linkage of the PBE+vdW method⁶ for intermolecular vdW interactions with the Lifshitz-Zaremba-Kohn theory³³ for the dielectric screening within the metal substrate. While the PBE+vdW^{surf} approach leads to accurate results in the asymptotic limit by construction, it uses a short-range damping function with one adjusted parameter. The optB88-vdW method is a modified version of the vdW-DF functional,⁵ by using an empirically optimized optB88-like exchange functional. Both PBE+vdW^{surf} and optB88-vdW methods can accurately describe intermolecular interactions with mean absolute relative errors on the order of 9%^{8,29} compared to coupled-cluster dimer binding energies for the S22 molecular database. Less is known about the performance of these methods for solids and weakly adsorbed molecules on surfaces, although encouraging results have been reported for a few condensed matter systems.^{10,11,32,34} It is important to benchmark the newly developed methods on a wider set of condensed matter systems, especially because the PBE+vdW^{surf} and optB88-vdW methods are based on very different approximations. For comparison purposes, calculations using the vdW-DF functional and its second version (vdW-DF2)³⁵ were also carried out for the Bz/Pt(111) and Bz/Au(111) systems.

The FHI-aims code was employed for the PBE+vdW^{surf}, PBE+vdW, PBE,³⁶ and local-density approximation (LDA) calculations. We used the “tight” settings, including the standard numerical atom-centered orbitals (NAO) basis set “tier2” for H and C, and “tier1” for transition metals. For all structural relaxations, we used a convergence criterion of 10^{-2} eVÅ⁻¹ for the maximum final force. Also a convergence criteria of 10^{-5} electrons for the electron density and 10^{-4} eV for the total energy of the system were utilized for all computations. The scaled zeroth-order regular approximation (ZORA) was applied for treating relativistic effects. Using these settings, the accuracy in determining the binding energy and equilibrium distance is better than 0.01 eV and 0.005 Å, respectively.

For bulk lattice constant calculations, we used a Monkhorst-Pack³⁷ grid of $16 \times 16 \times 16$ k -points. The lattice constants of the bulk metals have been obtained by using the Birch-Murnaghan equation of state fit to DFT cohesive energy curves.³⁸ Using the respective lattice constants from each method, we built up a 6-layer slabs with a (3×3) unit cell, with no reconstruction of Pt(111) and Au(111). Each slab was separated by a 20 Å vacuum. The vdW interactions between metal atoms were also considered when performing the relaxations. We constrained the bottom four metal layers while fully relaxed the molecule and the uppermost two metal layers during geometry relaxations. For slab calculations, we used a $6 \times 6 \times 1$ k -points mesh.

For the calculation of the binding curves, we changed the adsorption height d of Bz, which is evaluated relative to the position of the unrelaxed topmost metal layer. For each structure, we fixed the z coordinates of the carbon backbone and the metal atoms in the bottommost four of the employed six layer surface model.

The VASP code was employed for the optB88-vdW, vdW-DF, and vdW-DF2 calculations. Inner electrons replaced by the projector augmented wave (PAW) method, whilst the monoelectronic valence electrons were expanded in plane-waves with a $E_{\text{cut-off}} = 500$ eV. For slab calculations, we used a $4 \times 4 \times 1$ k -points mesh. For metal supercell, we used a (3×3) unit cell with 6 atomic layers (3 bottom layers fixed to the corresponding bulk optimal position for each method). Dipole correction was applied along the direction perpendicular to the metal surface. Geometry optimizations were performed with a residual force threshold of 0.03 eVÅ⁻¹.

III. RESULTS

The typical strongly bound Bz/Pt(111) system (adsorption energy 1.57-1.91 eV²⁸) and the typical weakly bound Bz/Au(111) system (adsorption energy 0.73-0.87 eV³⁹) are used first to demonstrate our point. Accurate experimental data is available for both of these systems, enabling direct quantitative verification of our theoretical calculations. To demonstrate the differences in the adsorption mechanism, we explore the potential-energy surface (PES) for Bz on the Pt(111) and Au(111) surfaces. We place a single Bz molecule at the eight high-symmetry adsorption sites of the (111) metal surface,⁴⁰ followed by geometry relaxation. The adsorption geometries and energies for Bz on Au(111) and Pt(111) at the preferable adsorption site are shown in Fig. 1 and Table I. Already here one can clearly distinguish the different nature of bonding for the adsorption of Bz on Pt(111) and Au(111). Irrespective of the functional used (PBE, PBE+vdW, and PBE+vdW^{surf}), the bri30° is the most preferable site for Bz/Pt(111), with an angle of 30° between the C–C and Pt–Pt bonds, see Fig. 1. This result is consistent with previous periodic slab GGA calculations,⁴⁰⁻⁴⁴ as well as low-energy electron diffraction

(LEED)⁴⁵ and scanning tunneling microscopy (STM)⁴⁶ experiments. Moreover, the PES shows a corrugation of 1.33 eV for Bz/Pt(111) when using PBE+vdW^{surf}. In contrast, the PES for Bz/Au(111) is found to be flat, with only 0.04 eV corrugation. This result further justifies the STM observations that even at a temperature of 4 K, Bz molecules are capable of diffusing over the Au(111) terraces.⁴⁷

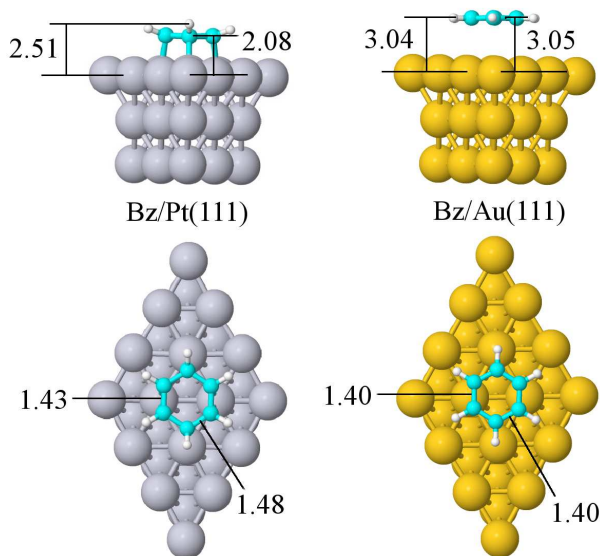


FIG. 1. Adsorption structures of the Bz/Pt(111) system and Bz/Au(111) system, both at the so-called bri30° adsorption site (see text). We carried out extended periodic calculations, but only a small part of the supercell is shown. Six metal layers were used but only the topmost three layers are depicted in the figure. The indicated distances (\AA) are obtained based on the PBE+vdW^{surf} optimized structures. Gray, yellow, cyan, and white spheres represent Pt, Au, C, and H atoms, respectively. Optimized lattice constants were used for every method.

The analysis of the equilibrium distances and adsorption energies in Table I demonstrates that both PBE+vdW^{surf} and optB88-vdW methods lead to an excellent agreement with the available experimental data. For the Bz/Pt(111) system, the PBE+vdW^{surf} adsorption energy of 1.96 eV is close to that from optB88-vdW (1.84 eV) and both methods agree with the measured calorimetry values at 0.7 ML (1.57-1.91 eV, the same coverage used for DFT calculations).²⁸ The PBE+vdW^{surf} adsorption energy converges to 2.18 eV with increasing surface cell size, within the error bar of calorimetry measurements in the limit of zero coverage (1.84-2.25 eV).²⁸ Note that the exclusion of the vdW interactions in the *strongly adsorbed* Bz/Pt(111) system would lead to a significant reduction in the binding energy (0.81 eV from PBE), in disagreement with the experimental data. The adsorption energies computed using the vdW-DF and vdW-DF2 methods are even smaller than those calculated with PBE. The adsorption energy for Bz adsorbed

TABLE I. Comparison of adsorption energy (E_{ad}) and average perpendicular heights (d_{CM} and d_{HM} for carbon-metal and hydrogen-metal, respectively) between DFT calculations and experimental data for Bz on Pt(111) and Au(111). The distances are referenced to the average positions of the relaxed topmost metal atoms. The adsorption energy E_{ad} is defined as $E_{\text{ad}} = -(E_{\text{AdSys}} - E_{\text{Me}} - E_{\text{Bz}})$, where the subscripts *AdSys*, *Me*, and *Bz* denote the adsorption system, the clean metal substrate, and the isolated Bz molecule, respectively.

System	Method	E_{ad} [eV]	d_{CM} [\AA]	d_{HM} [\AA]
Bz/Pt(111)	PBE+vdW ^{surf}	1.96	2.08	2.51
	optB88-vdW	1.84	2.12	2.53
	vdW-DF	0.77	2.16	2.57
	vdW-DF2	0.34	2.20	2.65
	PBE	0.81	2.10	2.54
	LDA	2.30	2.05	2.47
	Experiment	1.57-1.91 ^a	2.02±0.02 ^b	-
Bz/Au(111)	PBE+vdW ^{surf}	0.74	3.05	3.04
	optB88-vdW	0.79	3.23	3.23
	vdW-DF	0.59	3.44	3.42
	vdW-DF2	0.56	3.29	3.27
	PBE	0.15	3.62	3.62
	LDA	0.49	2.83	2.82
	Experiment	0.73-0.87 ^c	2.95-3.10 ^d	-

^a Heat of adsorption measured with calorimetry, at the same coverage (0.7 ML) used for the DFT calculations.²⁸ The error estimates of $\pm 10\%$ are taken from the reference.²⁸ Recent work suggests reduced errors of $\pm 5\%$.⁴⁸

^b LEED experiment.⁴⁵

^c TPD experiment.^{10,39}

^d Deduced data based on the experimental workfunction for Bz on Au(111) and adsorption distance for pentacene on Au(111).^{18,49,50}

on the Au(111) surface is considerably smaller than that of Bz/Pt(111). Also for Bz/Au(111), the PBE+vdW^{surf} adsorption energy (0.74 eV) agrees very well with both the optB88-vdW result (0.79 eV) and the experimental temperature-programmed desorption (TPD) data at 0.1 ML (0.73-0.87 eV).^{10,39} We conclude that PBE+vdW^{surf} and optB88-vdW methods yield quantitative agreement with experimental adsorption distances and energies for both weakly and strongly adsorbed Bz molecule. In contrast, LDA calculations are not systematic, underbinding for Au(111) and overbinding for Pt(111).

Deeper insight into the mechanism of Bz adsorption can be gained upon analysis of the binding energy curves, $E_{\text{ad}}(d)$, in Fig. 2. The binding energy curves exhibit several characteristic effects. With decreasing distance the binding energy of the adsorbate system increases, determined mainly by vdW interactions, and here (for $d > 3.5 \text{ \AA}$) Au(111) and Pt(111) show very similar behavior. In both cases the calculations show a small broadening of the energy levels. The fully occupied d -band of Au is obviously stiffer than the partially empty d -band of Pt. In fact, for the latter the Pauli repulsion can be weakened by the rearrangement of d -electron density (a similar effect has been investigated in previous literature¹⁹). As a consequence, the Bz molecule gets closer

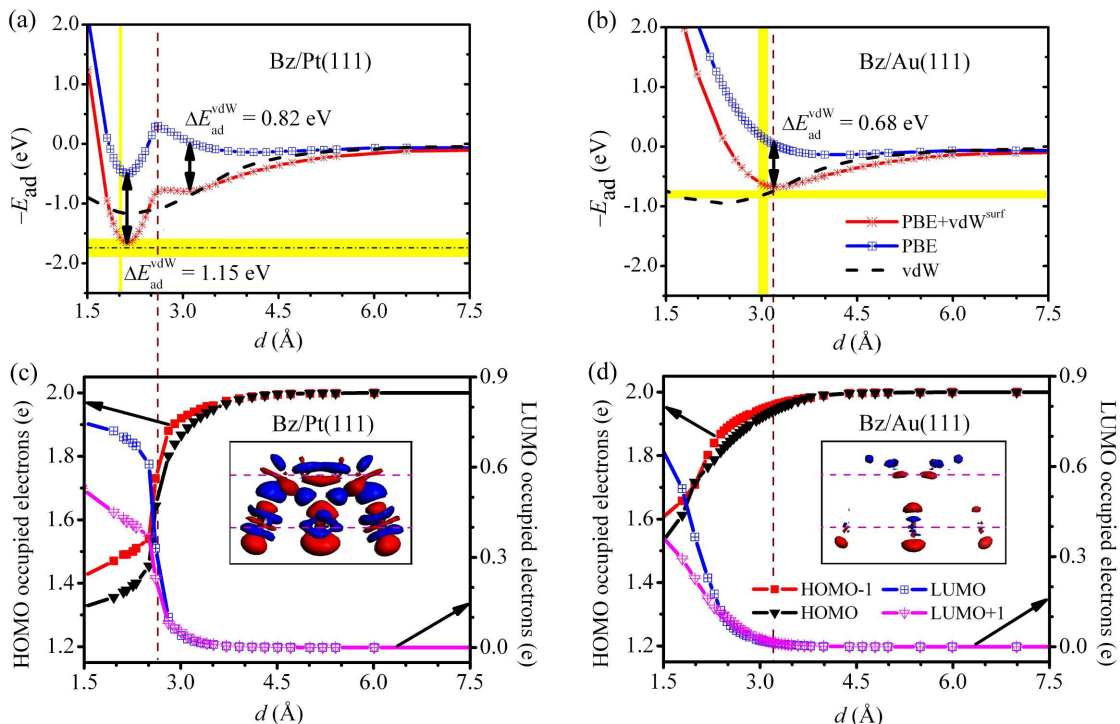


FIG. 2. Top: Adsorption energy $-E_{\text{ad}}$ as a function of the adsorption height d for Bz on Pt(111) (a) and on Au(111) (b) from the PBE and PBE+vdW^{surf} methods (the carbon backbone height d from the surface is kept fixed). The experimental binding distances and adsorption energies are indicated by yellow intervals. Bottom: Integrated projected molecular density of states⁵¹ for the HOMO-1, HOMO, LUMO, and LUMO+1 orbitals of the benzene molecule as a function of d for Bz on Pt(111) (c) and on Au(111) (d). The inset in panel (c) shows a side view of the electron density difference, which was obtained by subtracting electron density of isolated molecule and clean surface from an electron density plot of the entire adsorbed system, upon Bz adsorption on Pt(111) at $d=2.08$ Å (red = electron depletion, blue = electron accumulation). For the same value of the isosurface (0.04 \AA^{-3}), the electron density difference for Bz/Au(111) at $d=2.08$ Å is significantly weaker, see the inset in panel (d).

to the surface of Pt and the HOMO and LUMO levels of the combined system broaden and hybridize noticeably. This goes together with significant electron transfer: The HOMO and HOMO-1 orbitals of Bz molecule get partially depleted and the LUMO and LUMO+1 orbitals become partially filled. This behavior (broadening, shift, hybridization of levels, and electron transfer) is a clear signature of the covalent interaction for Bz/Pt(111). Thus, at the adsorption geometry the wave-function has attained a qualitatively new character. Figure 2 shows that this character change sets in for Pt at a distance of 3.1 Å. At 2.6 Å nearly a full electron has been transferred from the HOMO and HOMO-1 levels to the LUMO and LUMO+1 levels, and in the total energy we observe a “phase transition behavior” (cf. the peak at 2.6 Å). Finally, at the equilibrium geometry the electron transfer (rearrangement) is as large as ~ 1.1 electrons. For Au surface the process is much weaker and – not surprisingly – a covalent contribution to the adsorption process remains negligible. Thus, the vdW attraction governs the interaction.

Further inspection of the electron density difference at the strongly bound minimum for Bz/Pt(111) in Fig.

2(c) demonstrates the rather strong hybridization between the HOMO/LUMO orbitals of Bz and the d_{z^2} orbitals of the Pt(111) atoms. For the same adsorption height, the electron density difference for Bz/Au(111) is weak (see Fig. 2(d), inset). The presence of two minima for Bz/Pt(111) resembles the recently studied bonding of graphene on Ni(111).^{23,24} However, the adsorption of Bz on Pt(111) exhibits a different feature. In fact, Bz is exothermically bound on Pt(111) already when using PBE without vdW interactions, while the PBE adsorption energy is endothermic for graphene on Ni(111). Evidently, the functionalization of aromatic molecules would allow to control the position and stability of the two adsorption minima on metallic surfaces.

Interestingly, while covalency is crucial for the Bz/Pt(111) bonding character, energetically the vdW contribution is in fact significant. Upon inclusion of vdW interactions, the binding behavior is strongly modified – the barrier to adsorption vanishes, and a precursor physisorption state emerges for Bz/Pt(111). The PBE+vdW^{surf} method lowers the adsorption energy from 0.50 eV (pure PBE value) to 1.65 eV in Fig. 2. Thus the final adsorption results from a strongly concerted, syn-

TABLE II. Adsorption energies E_{ad} (eV) of Bz adsorbed on (111) surfaces of Ag, Pd, Rh, and Ir.

System	PBE	PBE+vdW ^{surf}	optB88-vdW
Bz/Ag(111)	0.09	0.75	0.72
Bz/Pd(111)	1.17	2.14	1.91
Bz/Rh(111)	1.48	2.52	2.27
Bz/Ir(111)	1.10	2.24	2.09

ergistic effort. Upon comparing the binding curves for Bz/Pt(111) and Bz/Au(111) we see that the vdW contribution (due to vdW^{surf}) for Bz/Pt(111), 1.15 eV, is even stronger than that for Bz/Au(111), 0.68 eV. The screened Bz/surface C_3 vdW coefficient is essentially the same for Pt(111) and Au(111) surfaces (2.17 and 2.02 hartree bohr³, respectively). Therefore, we conclude that the larger contribution of the vdW energy in the case of covalent bonding comes from the rather short adsorption distance of the Bz molecule from the surface.

Our conclusions hold in general for the adsorption of Bz on other transition metal surfaces. For Bz/Ir(111), the binding curve shows the same characteristic features as for Bz/Pt(111) in Fig. 2. For Bz adsorbed on the Pd(111), Rh(111), and Ir(111) surfaces, the vdW energy contributions from the PBE+vdW^{surf} method are in the range of 0.97-1.21 eV, greater than those for Bz physisorbed on Ag(111) and Au(111) (0.68-0.82 eV). Even larger vdW energies are found in more complex polyaromatic adsorption systems. For instance, the vdW energy is determined to be 1.77 eV for naphthalene (C₁₀H₈) on the Pt(111) surface with (5 × 4) unit cell. Also for this case the calculated adsorption energy from PBE+vdW^{surf} (2.91 eV) is within the experimental error bars (2.80-3.42 eV).⁵² For anthracene (C₁₄H₁₀) on

the Pt(111) surface with (6 × 4) unit cell, the adsorption energy contributed by vdW interactions (2.42 eV) largely exceeds that determined from the PBE functional (1.38 eV).

IV. CONCLUSION

In summary, we have demonstrated that the inclusion of vdW interactions qualitatively changes the adsorption behavior for benzene strongly interacting with (111) metal surfaces. The vdW energy in Bz/Pt(111), a typical strongly adsorbed system, is almost 0.5 eV greater than that in Bz/Au(111), a typical physisorbed system. The bonding mechanism of Bz/Pt(111) stems from a synergistic effort of covalent bonding and vdW interactions, and it is characterized by a peculiar “phase transition” behavior in the projected HOMO/LUMO occupations of the benzene molecule. Our findings for Bz adsorbed on Ag, Au, Pt, Pd, Rh, and Ir surfaces indicate that DFT calculations with dispersion interactions are essential for both weakly and strongly bound molecules on surfaces.

ACKNOWLEDGMENTS

We are grateful for support from the FP7 Marie Curie Actions of the European Commission, via the Initial Training Network SMALL (MCITN-238804). W.L. was funded by a fellowship from the Alexander von Humboldt Foundation. A.T. acknowledges support from the European Research Council (ERC Starting Grant VDW-CMAT). A.M. is supported by the ERC (ERC Starting Grant QUANTUMCRASS) and by the Royal Society through a Wolfson Research Merit Award. J.C. is a Ramón y Cajal fellow supported by the Spanish Government.

* tkatchenko@fhi-berlin.mpg.de
¹ F. S. Tautz, Prog. Surf. Sci. **82**, 479 (2007)
² P. Gomez-Romero, Adv. Mater. **13**, 163 (2001)
³ S. J. Jenkins, Proc. R. Soc. A **465**, 2949 (2009)
⁴ L. Kronik and N. Koch, MRS Bull. **35**, 417 (2010)
⁵ M. Dion, H. Rydberg, E. Schröder, D. C. Langreth, and B. I. Lundqvist, Phys. Rev. Lett. **92**, 246401 (2004)
⁶ A. Tkatchenko and M. Scheffler, Phys. Rev. Lett. **102**, 073005 (2009)
⁷ S. Grimme, J. Antony, S. Ehrlich, and H. Krieg, J. Chem. Phys. **132**, 154104 (2010)
⁸ J. Klimeš, D. R. Bowler, and A. Michaelides, J. Phys.: Condens. Matter **22**, 022201 (2010)
⁹ A. Tkatchenko, L. Romaner, O. T. Hofmann, E. Zojer, C. Ambrosch-Draxl, and M. Scheffler, MRS Bulletin **35**, 435 (2010)
¹⁰ V. G. Ruiz, W. Liu, E. Zojer, M. Scheffler, and A. Tkatchenko, Phys. Rev. Lett. **108**, 146103 (2012)
¹¹ J. Carrasco, B. Santra, J. Klimeš, and A. Michaelides, Phys. Rev. Lett. **106**, 026101 (2011)
¹² Busse, C *et al.*, Phys. Rev. Lett. **107**, 036101 (2011)

¹³ I. Hamada and M. Tsukada, Phys. Rev. B **83**, 245437 (2011)
¹⁴ A. K. Kelkkanen, B. I. Lundqvist, and J. K. Nørskov, Phys. Rev. B **83**, 113401 (2011)
¹⁵ M. Vanin, J. J. Mortensen, A. K. Kelkkanen, J. M. Garcia-Lastra, K. S. Thygesen, and K. W. Jacobsen, Phys. Rev. B **81**, 081408 (2010)
¹⁶ K. Toyoda, I. Hamada, K. Lee, S. Yanagisawa, and Y. Morikawa, J. Chem. Phys. **132**, 134703 (2010)
¹⁷ J. Wellendorff, A. Kelkkanen, J. J. Mortensen, B. I. Lundqvist, and T. Bligaard, Top. Catal. **53**, 378 (2010)
¹⁸ E. Abad, Y. J. Dappe, J. I. Martínez, F. Flores, and J. Ortega, J. Chem. Phys. **134**, 044701 (2011)
¹⁹ J. L. F. Da Silva, C. Stampfl, and M. Scheffler, Phys. Rev. Lett. **90**, 066104 (2003)
²⁰ D. L. Chen, W. A. Al-Saidi, and J. K. Johnson, Phys. Rev. B **84**, 241405 (2011)
²¹ P. L. Silvestrelli, A. Ambrosetti, S. Grubisic, and F. Ancilotto, Phys. Rev. B **85**, 165405 (2012)
²² N. Atodiresei, V. Caciuc, P. Lazic, and S. Blügel, Phys. Rev. Lett. **102**, 136809 (2009)

- ²³ F. Mittendorfer, A. Garhofer, J. Redinger, J. Klimeš, J. Harl, and G. Kresse, *Phys. Rev. B* **84**, 201401 (2011)
- ²⁴ X. Li, J. Feng, E. Wang, S. Meng, J. Klimeš, and A. Michaelides, *Phys. Rev. B* **85**, 085425 (2012)
- ²⁵ W. Liu, A. Savara, X. Ren, W. Ludwig, K.-H. Dostert, S. Schauermann, A. Tkatchenko, H.-J. Freund, and M. Scheffler, *J. Phys. Chem. Lett.* **3**, 582 (2012)
- ²⁶ K. Johnston, J. Kleis, B. I. Lundqvist, and R. M. Nieminen, *Phys. Rev. B* **77**, 121404 (2008)
- ²⁷ H.-J. Kim, A. Tkatchenko, J.-H. Cho, and M. Scheffler, *Phys. Rev. B* **85**, 041403 (2012)
- ²⁸ H. Ihm, H. M. Ajo, J. M. Gottfried, P. Bera, and C. T. Campbell, *J. Phys. Chem. B* **108**, 14627 (2004)
- ²⁹ A. Tkatchenko, R. A. DiStasio, Jr., R. Car, and M. Scheffler, *Phys. Rev. Lett.* **108**, 236402 (2012)
- ³⁰ V. Blum, R. Gehrke, F. Hanke, P. Havu, V. Havu, X. Ren, K. Reuter, and M. Scheffler, *Comp. Phys. Comm.* **180**, 2175 (2009)
- ³¹ G. Kresse and J. Furthmüller, *Phys. Rev. B* **54**, 11169 (1996)
- ³² J. Klimeš, D. R. Bowler, and A. Michaelides, *Phys. Rev. B* **83**, 195131 (2011)
- ³³ E. Zaremba and W. Kohn, *Phys. Rev. B* **13**, 2270 (1976)
- ³⁴ G. X. Zhang, A. Tkatchenko, J. Paier, H. Appel, and M. Scheffler, *Phys. Rev. Lett.* **107**, 245501 (2011)
- ³⁵ K. Lee, E. D. Murray, L. Kong, B. I. Lundqvist, and D. C. Langreth, *Phys. Rev. B* **82**, 081101 (2010)
- ³⁶ J. Perdew, K. Burke, and M. Ernzerhof, *Phys. Rev. Lett.* **77**, 3865 (1996)
- ³⁷ H. J. Monkhorst and J. D. Pack, *Phys. Rev. B* **50**, 17953 (1976)
- ³⁸ F. Birch, *Phys. Rev.* **71**, 809 (1947)
- ³⁹ D. Syomin, J. Kim, B. E. Koel, and G. B. Ellison, *J. Phys. Chem. B* **105**, 8387 (2001)
- ⁴⁰ M. Saeys, M. F. Reyniers, G. B. Marin, and M. Neurock, *J. Phys. Chem. B* **106**, 7489 (2002)
- ⁴¹ M. Saeys, M. F. Reyniers, M. Neurock, and G. B. Marin, *J. Phys. Chem. B* **107**, 3844 (2003)
- ⁴² F. Mittendorfer, C. Thomazeau, P. Raybaud, and H. Toulhoat, *J. Phys. Chem. B* **107**, 12287 (2003)
- ⁴³ C. Morin, D. Simon, and P. Sautet, *J. Phys. Chem. B* **108**, 5653 (2004)
- ⁴⁴ W. Gao, W. Zheng, and Q. Jiang, *J. Chem. Phys.* **129**, 164705 (2008)
- ⁴⁵ A. Wander, G. Held, R. Q. Hwang, G. S. Blackman, M. L. Xu, P. de Andres, M. A. Van Hove, and G. A. Somorjai, *Surf. Sci.* **249**, 21 (1991)
- ⁴⁶ P. S. Weiss and D. M. Eigler, *Phys. Rev. Lett.* **71**, 3139 (1993)
- ⁴⁷ B. A. Mantooth, E. C. H. Sykes, P. Han, A. M. Moore, Z. J. Donhauser, V. H. Crespi, and P. S. Weiss, *J. Phys. Chem. C* **111**, 6167 (2007)
- ⁴⁸ W. Lew, M. C. Crowe, E. Karp, O. Lytken, J. A. Farmer, L. Árnadóttir, C. Schoenbaum, and C. T. Campbell, *J. Phys. Chem. C* **115**, 11586 (2011)
- ⁴⁹ K. Toyoda, Y. Nakano, I. Hamada, K. Lee, S. Yanagisawa, and Y. Morikawa, *Surf. Sci.* **603**, 2912 (2009)
- ⁵⁰ E. Abad, J. Ortega, Y. J. Dappe, and F. Flores, *Appl. Phys. A* **95**, 119 (2009)
- ⁵¹ G. M. Rangger, L. Romaner, G. Heimel, and E. Zojer, *Surf. Interface Anal.* **40**, 371 (2008)
- ⁵² J. M. Gottfried, E. K. Vestergaard, P. Bera, and C. T. Campbell, *J. Phys. Chem. B* **110**, 17539 (2006)